ELSEVIER

Bioelectrochemistry 58 (2002) 137–147

Bioelectrochemistry

www.elsevier.com/locate/bioelechem

The influence of promoter and of electrode material on the cyclic voltammetry of *Pisum sativum* plastocyanin

D.L. Johnson, C.J. Maxwell, D. Losic, J.G. Shapter, L.L. Martin *

Chemistry (SOCPES), Flinders University, Adelaide, SA 5001, Australia

Received 26 March 2002; received in revised form 27 May 2002; accepted 4 June 2002

Abstract

The reversible cyclic voltammetry of pea plastocyanin (*Pisum sativum*) was studied with a wide range of electrodes: edge-oriented pyrolytic graphite (PGE), glassy carbon (GCE), gold (Au) and platinum (Pt) electrodes. Plastocyanin was coated onto the electrode surface by exploiting the electrostatic interaction between the negatively charged protein and a wide range of positively charged promoters. The effect of the redox response with an extended range of promoters, including poly-L-lysine, polymyxin B, neomycin, tobramycin, geneticin, spermine and spermidine, were included in this study. The resulting cyclic voltammograms reveal that the observed midpoint potential for plastocyanin can be shifted significantly depending on the choice of promoter. The stability of the negatively charged plastocyanin–promoter layer on an electrode was gauged by the rate of bulk diffusion of the protein from the immobilised film into the solution. Reversible cyclic voltammograms were obtained using edge-oriented pyrolytic graphite (PGE) and glassy carbon electrodes (GCE) with all promoters; however, platinum and gold electrodes were unable to sustain a defined redox response. The combination of pyrolytic graphite electrode/poly-L-lysine/plastocyanin was found to be the most stable combination, with a redox response which remained well defined in solution for more than 1 h at pH 7.0. The midpoint potentials obtained in this manner differed between the two graphite electrodes PGE and GCE using poly-L-lysine as the promoter. This effect was in addition to the expected pH dependence of the midpoint potential for plastocyanin and the results indicated that the pK_a for plastocyanin on PGE was 4.94 compared to that on GCE of 4.66. It is concluded that both the electrode material and the nature of the promoter can influence the position of the redox potentials for proteins measured in vitro.

This study extends the range of biogenic promoters used in combination with electrode materials. Thus, we can begin to develop a more comprehensive understanding of electrode–protein interactions and draw conclusions as to metalloprotein function, in vivo. To support these studies, we have sought information as to the nature of the electrode/promoter/protein interaction using scanning tunneling microscopy (STM) to study both the promoter and the plastocyanin protein on a gold surface.

Keywords: Plastocyanin; Redox potential; Promoters; Cyclic voltammetry; Metalloproteins; Scanning tunneling microscopy

1. Introduction

Direct protein electrochemistry techniques have provided valuable tools for the identification of redox signatures for many metalloproteins [1–4]. Despite advances in the technical aspects of measuring low currents and baseline compensation programs, many deficiencies remain in our understanding of the respective influences of electrodes, promoters and the proteins themselves on the redox response. Detailed studies have been carried out for both positively and negatively charged, low-molecular weight, electron transfer metalloproteins, such as ferredoxins [2–6], cyctochrome *c* [4] and plastocyanin [7]. Convincing evidence is presented that the choice of promoter used for these experiments can significantly influence the thermodynamics of the electron transfer reaction and, hence, affect the measured reduction potentials [7,8]. For cytochrome b_5, both the promoter, poly-L-lysine or $[Cr(NH_3)_6]^{3+}$ and the Mg^{2+} ion concentration can produce shifts of the half-wave potential by as much as 60 mV [9]. Similar studies with plastocyanin have demonstrated that varying Mg^{2+} ion concentrations can shift the reduction potential, although

Abbreviations: MES, 2-(*N*-morpholino)ethanesulfonic acid; HEPES, *N*-(2-hydroxyethyl)piperazine-*N*′-(ethanesulfonic acid); TAPS, *N*-tris(hydroxymethyl)methyl-3-aminopropanesulfonic acid; EGTA, ethylene glycol-bis(β-aminoethyl ether)-*N*,*N*,*N*′,*N*′-tetraacetic acid; PGE, edge-oriented pyrolytic graphite electrode; GCE, glassy carbon electrode.

* Corresponding author. Tel.: +61-8-8201-2465; fax: +61-8-8201-2905.
E-mail address: Lisa.Martin@Flinders.edu.au (L.L. Martin).

1567-5394/02/$ - see front matter © 2002 Elsevier Science B.V. All rights reserved.
PII: S1567-5394(02)00125-1

ionic strength effects were negligible [7,8]. These workers [7,8] obtained well-defined responses with a pyrolytic graphite electrode (edge-oriented), PGE, but not with a glassy carbon electrode, GCE, under their experimental conditions, although other studies [10] were able to elicit a response using modified gold electrodes. However, to date, no study of the electrode dependence has been carried out, and furthermore, the range of promoters used has been limited.

Plastocyanin is a member of the Blue Copper family of electron transfer proteins. This mobile protein shuttles between the *bf*-complex and Photosystem I (PSI), thereby enabling the photosynthetic electron transfer process between PSI and PSII to be efficiently achieved [11]. The active site for plastocyanin contains a single "type-1" copper ion, such that the oxidised Cu^{II} can be reduced to Cu^{I}, reversibly. Extensive structural [11], spectroscopic [11,12] and reactivity studies [7,11,13,14] for plastocyanin have provided a good understanding of the molecular characteristics of this protein, thus making it an ideal candidate for an in vitro examination of the factors that could affect its redox response during photosynthesis.

Redox studies with plastocyanins isolated from higher plants, such as spinach (*Spinacea oleracea*) and poplar (*Populus nigra*), show unusually high reduction potentials of 389 ± 7 mV, whereas plastocyanin from blue-green algae (*Anabaena variabilis*) are lower (318 ± 3 mV) [7,13,15]. In addition, the redox response is influenced by pH [7,10,16–18], surface charge [18,19] and Mg^{2+} concentration [7,17]. These studies confirm that a range of experimental factors can influence the interfacial properties, hence, the reported redox potential for plastocyanin.

Electrode modification is typically required in order to observe reversible voltammetry of metalloproteins [1–3]. Thus, reliable electrochemical responses can be observed for negatively charged electron transfer proteins, such as plastocyanin, ferredoxins and cytochromes by using direct promotion methods. In particular, reversible data can often be obtained at pyrolytic graphite (edge oriented and basal plane), glassy carbon, gold or platinum electrodes, in the presence of "promoters" to co-adsorb the protein [2,3]. However, these electrochemical data are often reported using only one type of promoter thereby precluding comparisons to other studies that employed different promoters under similar conditions. Clearly, there is a need to systematically define the influence of common promoters and electrodes in order to compare and correlate redox data obtained in vivo with metalloproteins and enzymes. Furthermore, the contribution that a particular promoter may have on the electrochemical response is yet to be systematically explored.

Recent studies indicate that the method of promotion along with shifts in protein peak potential correlate with the promoter type and concentration [8]. Similar shifts are expected for electrostatically immobilised systems where a promoter/protein sample is prepared prior to being placed into a buffered solution [5,6,8]. This mode of protein attachment is through electrostatic attraction, which leads to bulk diffusion of the sample away from the electrode at a rate defined by the degree of attraction between the promoter and the protein.

This present study reports the cyclic voltammetry obtained for several promoters using monolayer films of *Pisum sativum* plastocyanin on pyrolytic graphite, glassy carbon, gold and platinum electrodes. It examines (i) their ability to facilitate plastocyanin electron transfer and (ii) to determine the extent of electrostatic interaction between the promoter and the protein. Of particular interest here is the polymerised form of the naturally occurring L-lysine (poly-L-lysine), which has been used in other studies with considerable success [8,20,21], although six other promoters are also employed here. The influence of the electrode material on the redox response (both current and midpoint potential) is another variable we have addressed. The electrochemical response is often dependant on the nature and surface condition of the electrode, for instance, C–O functionalities on the edge-oriented pyrolytic graphite electrode are often exploited in the quest for a reversible response for positively charged proteins. Finally, we have examined the interface between the promoter, poly-L-lysine and the electrode by scanning tunneling microscopy (STM). Although this technique was recently reviewed [22], we cannot find any other study of plastocyanin using STM. We also believe that this is the first comprehensive study of plastocyanin using these four electrode materials and with such a wide range of promoters.

2. Experimental

2.1. Source, isolation and purification

Plastocyanin was isolated from 21-day-old pea (*P. sativum*) leaves and purified as described elsewhere [23]. The A_{280}/A_{597} ratio for the experimental sample was 10:1 at the calculated concentration 5×10^{-4} M (ε_{597} was assumed to be 4500 M^{-1} cm^{-1}).

2.2. Materials and instrumentation for electrochemical experiments

All chemicals were reagent grade and used without further purification. Poly-L-lysine (MW 150–300 kDa) was purchased from Sigma as a 0.1% aqueous solution. Milli-Q water was used both as a solvent and in all rinsing steps. Aqueous solutions were buffered in the pH range 4.5–8.5 using a buffer mixture containing 5 mM of MES, HEPES, TAPS and 0.1 mM EGTA. The pH was determined using a calibrated Orion 290A pH meter. The solution volume was 15 ml and the supporting electrolyte was 0.1 M NaCl (99%). The bulk solution was changed after each fresh application of the promoter/protein to the electrode to

avoid the influence of dissolved molecules during experiments. Dissolved oxygen was removed by purging with nitrogen through solutions for 10 min prior to the experiment and a stream of nitrogen was maintained over the solution during all experiments. Cyclic voltammograms were recorded using a Bioanalytical Systems (BAS) Model C3 Cell stand linked to a BAS Model 100B electrochemical analyser, all measurements were made in triplicate, and data were obtained at scan rates between 0.02 and 0.5 V s^{-1} at 22 ± 1 C. Voltametric data were obtained using (i) an edge-oriented pyrolytic graphite electrode (radius 2.0 mm), (ii) a glassy carbon electrode (radius 1.9 mm), (iii) a platinum electrode (radius 1.2 mm) or (iv) a gold electrode (radius 1.2 mm). Electrodes were purchased from BAS except for the PGE electrode, which was prepared according to published methods [5,6]. Prior to each experiment, the electrode surface was polished with alumina–water slurry (alumina particle size 0.3 μm), washed with Milli-Q water and sonicated for 1 min. The reference and counter electrodes were Ag/AgCl (3 M NaCl) and platinum wire, respectively. The reference electrode was calibrated against the $[Fe(CN)_6]^{3-/4-}$ couple and was measured before and after each experiment to check for potential drifting. The maximum variation noted was 5 mV and the experimental data were adjusted accordingly. Midpoint potentials for reversible processes were calculated as the midpoint of the oxidation (E_{pa}) and reduction (E_{pc}) peaks and peak separation and reported as ΔE. All data are reported versus the normal hydrogen electrode (NHE).

Two experimental methods were used to apply the promoter and the protein to the electrode surface.

2.2.1. Method 1: dry–dry method (DDM)

A buffered solution at the required pH was placed into the electrochemical cell and deoxygenated for 10 min. An aqueous solution of the appropriate promoter (10 μl of 0.02 M) was placed on the working electrode and allowed to evaporate with gentle warming. Plastocyanin (10 μl of a 5×10^{-4} M sample) was then applied and allowed to evaporate slowly at room temperature. The electrode was then placed in the buffered solution and voltametric scans recorded immediately. Both the anodic and cathodic peak currents were measured for all scans and the ratios found to be $\sim$1:1.

2.2.2. Method 2: dry–wet method (DWM)

This method differed only slightly from that described above. Following the coating of the electrode with the promoter, plastocyanin (10 μl of a 5×10^{-4} M sample) was immediately applied on to the working electrode. The electrode was immediately placed into the buffer solution in the electrochemical cell and cyclic voltammograms were recorded. The protein coating was less stable on the electrode using this method as assessed with Method 1 where fewer scans were achieved due to rapid diffusion of the immobilised plastocyanin into the buffer solution. Scan direction was particularly relevant with this method as diffusion of the protein into the solution invariably led to a larger forward than reverse current. The currents reported were obtained from the peak maxima during experiments starting at 0 V and scanning anodically and returning to 0 V. The anodic currents obtained by this method were consistently higher than those of the corresponding cathodic waves because of the poorly immobilised promoter noted above.

Reproducible results were obtained using Method 1, and data reported here were all obtained with this method.

3. Scanning tunneling microscopy

STM images of samples were obtained in air with a Digital Nanoscope II microscope using tungsten tips in both height and current mode. Atomically flat gold electrodes were prepared as previously described [24]. Images were obtained with current of <2 A and a tip bias voltage of <1 V. Poly-L-lysine samples were prepared by the addition of a 0.01% w/v aqueous solution to the gold surface followed by evaporation. Protein samples were prepared using Method 1 and buffer salts were removed by gentle washing with water. Routinely, five different areas on at least three different samples were examined for reproducibility.

4. Results

4.1. Influence of electrode material on voltametric response and midpoint potential

Reversible voltammograms with well-defined peak shapes were observed for plastocyanin physisorbed at both PGE and GCE electrodes using poly-L-lysine as a promoter. No significant response was detected at either the gold or platinum electrodes under similar conditions. Fig. 1 compares these results for plastocyanin protein physisorbed onto the poly-L-lysine promoter at all electrodes used in this study: PGE, GCE, platinum and gold.

These data confirm the findings from other workers [8] that negatively charged proteins interact favorably with poly-L-lysine at the PGE. In addition, we obtained a well-defined, reversible redox couple for plastocyanin at GCE, although a significant electrode dependence of the midpoint potential was observed. The E_{mid} value obtained at the PGE was 15 mV more positive than that observed at the GCE. Each experiment was repeated at least three times on different occasions and the variation in response was less than 4 mV. Although the midpoint potential varies with the two carbon electrodes, the peak separation, ΔE remained constant at 50–60 mV expected for a mixture of finite and infinite diffusion [1].

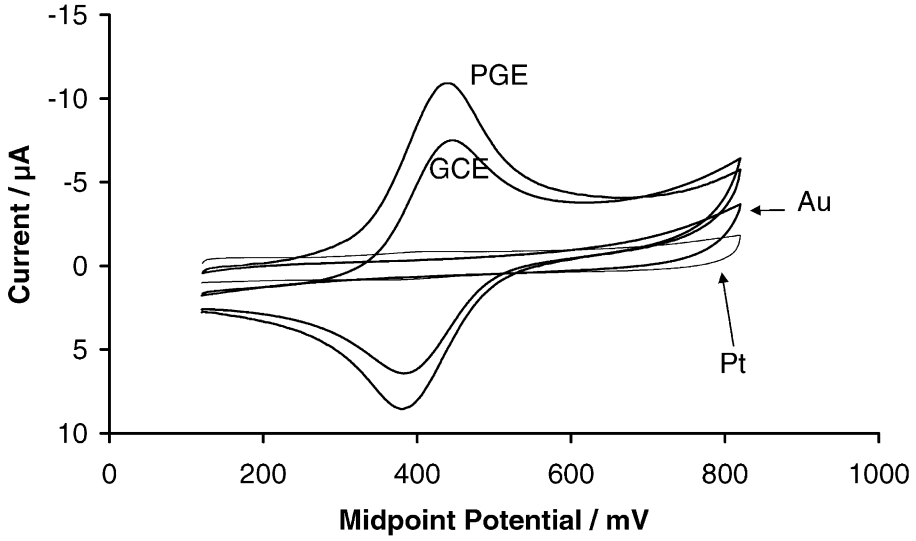

Fig. 1. Cyclic voltammetry of plastocyanin at PGE, GCE, gold and platinum electrodes promoted using poly-L-lysine. Scan rate was 200 mV/s.

4.2. Influence of promoter type on the peak potential

The variation of the midpoint potential with different promoter types for the direct electrochemistry of metalloproteins has been noted by several workers [7,8]. Although to date no systematic study has been undertaken to examine this effect with a wide range of potential promoters, the present work re-examines some work from earlier publications. We have comprehensively assessed this effect for a wide range of positively charged promoters where electrostatic attachment of plastocyanin to PGE occurs. Fig. 2 illustrates these results for these promoters which are all biogenic polyamines. For each promoter, a well-defined reversible voltametric response was observed with $\Delta E \sim 60$ mV although, as indicated, significant shifts in midpoint potentials were observed. The lowest value for the midpoint potential was found for geneticin, with 395 ± 4 mV, and the highest value of 406 ± 4 mV found for neomycin (Table 1). An average for these values coincided with that measured with poly-L-lysine, of 401 ± 4 mV.

4.3. PGE/poly-L-lysine/plastocyanin combination

Reversible cyclic voltammograms were obtained for plastocyanin with all promoters using Method 1. Using Method 2, the protein film was less stable and the ratio of

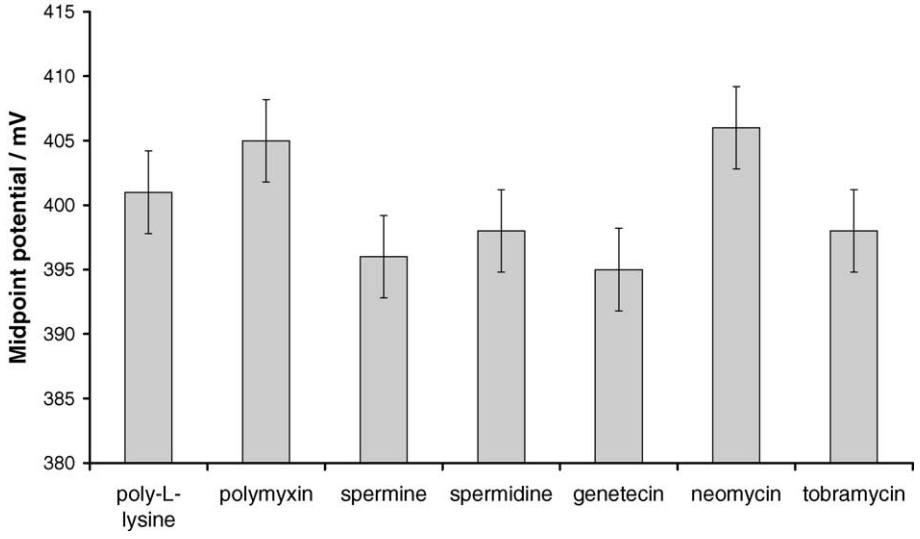

Fig. 2. The influence of promoter on midpoint potential using PGE. All values were obtained in triplicate and the midpoint potentials shown are the average values, with a reproducibility of ± 4 mV. Scan rate was 200 mV/s.

Table 1
Influence of promoter on midpoint potentials, E_{mid}, and peak separation, ΔE, for plastocyanin on PGE

Promoter	Midpoint potential, E_{mid} (mV) vs. NHE	Peak separation, ΔE (mV)
Poly-L-lysine	401	49
Polymyxin	405	50
Spermine	396	55
Spermidine	398	54
Geneticin	395	56
Neomycin	406	50
Tobramycin	398	57

Scan rate was 200 mV/s.

peak currents (i_{pa}/i_{pc}) was always greater than 1 due to fast dissolution of the protein into the buffer solution. The combination of protein/promoter/electrode for plastocyanin was assessed for a PGE modified using poly-L-lysine resulting in the well-defined voltammograms shown in Fig. 3a. In addition, the observed peak potential was independent of scan rate over the range 0.02–0.5 V s^{-1}. Furthermore, Fig. 3b shows that both anodic and cathodic peak currents, i_p, were linear when plotted against $v^{1/2}$ over the same range of scan rates. Peak separations, ΔE, were all between 50 and 60 mV.

This is an interesting result suggesting that plastocyanin is immobilised at the electrode interface so that diffusion of outer layers of weakly bound protein occurs at a consistent rate and provides sufficient protein in the bulk solution to effect the response expected for conventional diffusion controlled electron transfer. The peak separations were consistent with the combination of semi-infinite (mass transport) and finite (immobilised) diffusion processes occurring.

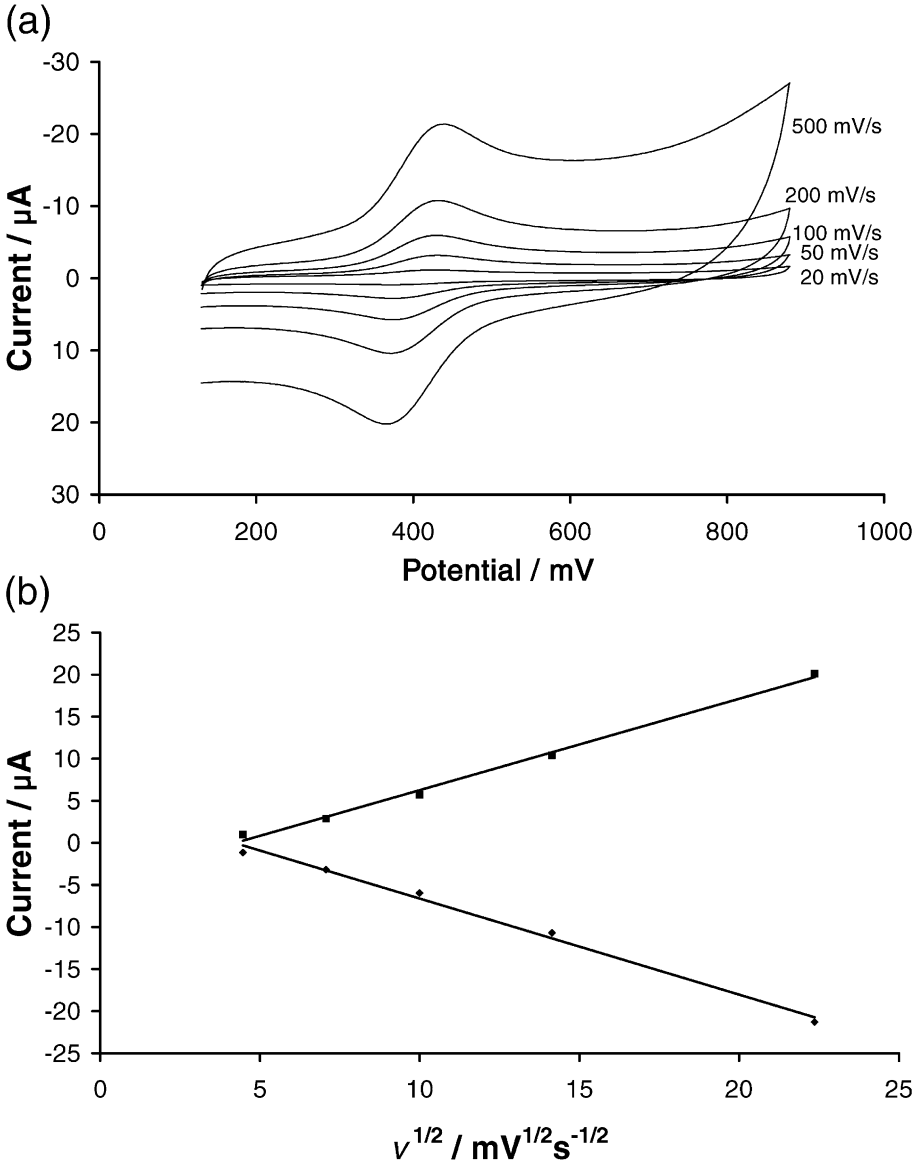

Fig. 3. Scan rate dependence of plastocyanin on (a) PGE using poly-L-lysine promoter. (b) The linear dependence of the peak currents for both forward and reverse waves, $\Delta E_p \sim 60$ mV.

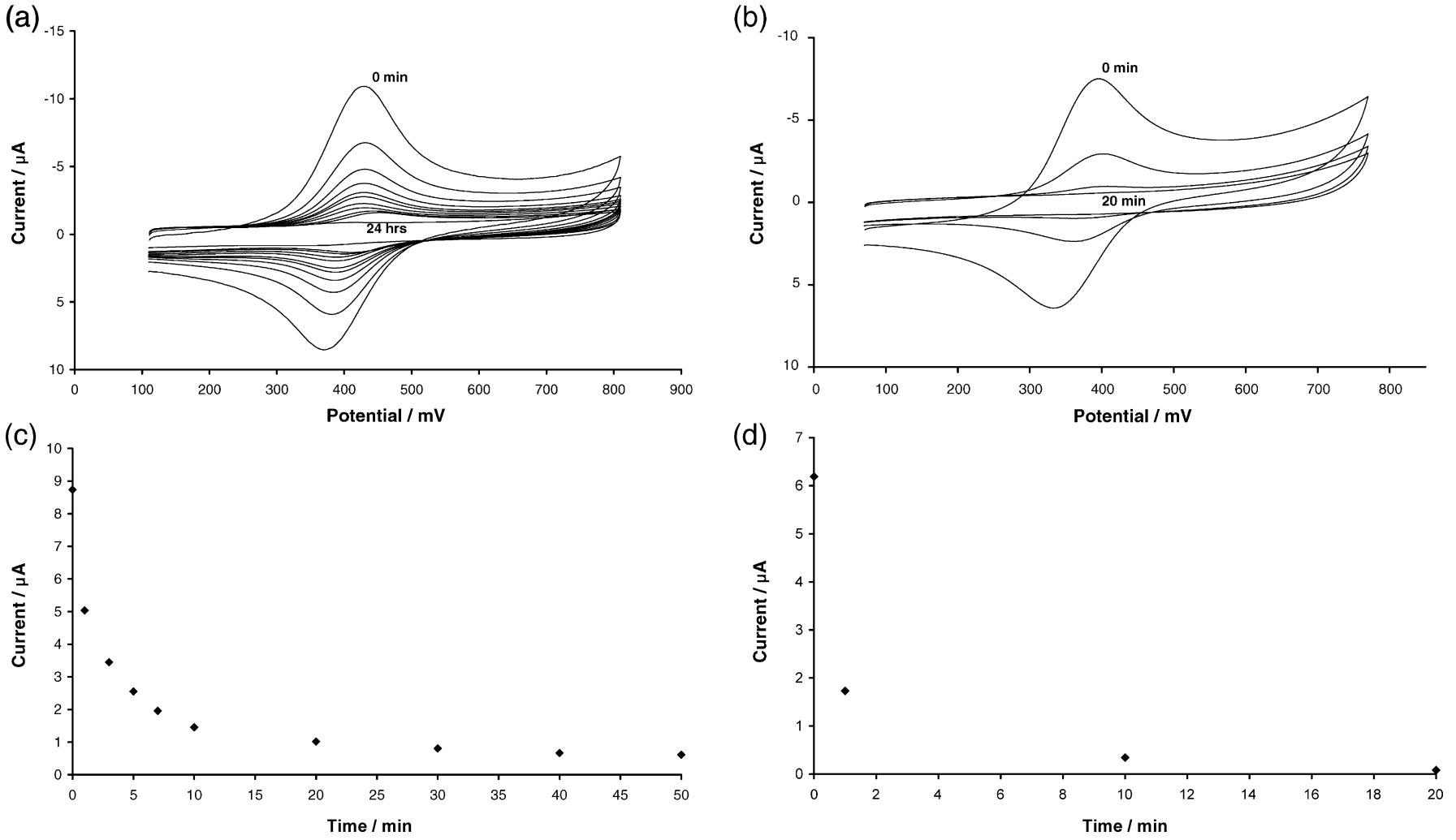

Fig. 4. The stability of plastocyanin/poly-L-lysine interaction with time using poly-L-lysine promoter on (a) PGE at 0, 1, 3, 5, 7, 10, 20, 30, 40, 50 min, and 24 h (outer to inner scans) and (b) GCE at 0, 1, 10 and 20 min (outer to inner scans). (c) and (d) represent the cathodic peak current versus time for the respective electrodes (a) and (b).

4.4. Stability of the poly-L-lysine/plastocyanin film at carbon electrodes

The stability of the protein layer immobilised on pyrolytic and glassy carbon electrodes through electrostatic attachment by poly-L-lysine is seen in Fig. 4a and b, respectively. No voltametric response was observed with the buffer solution containing only electrolyte. The voltammograms in Fig. 4a show that the PGE/poly-L-lysine/plastocyanin combination was significantly more stable than GCE/poly-L-lysine/plastocyanin, with a peak shape consistent with linear diffusion, well defined up to 1 h. The large decrease in initial current was attributed to the excess protein, not in direct contact with the promoter "washing off" the electrode. This conclusion, rather than denaturation of the protein, is supported by the sharp decrease in current versus time followed by an insignificant change in current over 10–60 min, resulting from the immobilised protein layer (insets in Fig. 4a and b).

The stability of the protein/poly-L-lysine at the GCE (Fig. 4b) is much less than at the PGE (Fig. 4a). Presumably, the pyrolytic graphite surface attracts the promoter less effectively, and thus, the protein signal reduces to ca. a quarter of the original intensity within the first few minutes and only a poorly defined wave is evident after 10 min.

4.5. Influence of electrode material on the pH dependence of E_{mid}

In its oxidised form (Cu^{II}), the X-ray crystal structure of plastocyanin is independent of pH [11]. However, the reduction from Cu^{II} to Cu^{I} at low pH leads to a change in stereochemistry due to the protonation of a histidine coordinated to a copper ion at the active site [11]. Not surprisingly, this protonation equilibria for plastocyanin is reflected in the redox response [7]. The influence of electrode material on the pH dependence was investigated here, as there is little quantitative data reported on this dependence [2]. Fig. 5 illustrates the midpoint potential shift with pH for the two carbon electrodes, PGE and GCE, which provided strong redox responses in the presence of poly-L-lysine.

As noted earlier, the midpoint potentials obtained with PGE are shifted anodically when compared to those obtained at GCE. The pH dependence of E_{mid} for these waves was determined over the range pH 4.0–8.5. The data obtained for both electrodes show similar pH profiles, and can be well reproduced by a square reaction scheme where the reduced form of plastocyanin is protonated at low pH [1,7]. The quality of fit of these data to $E^{\circ\prime}_{obs}=E'_{alk}+(2.303RT/F)\log(1+[H^+]/K_H)$ is illustrated in Fig. 5 where the parameters of best fit for the reduced plastocyanin are $K_H=1.16\times10^{-5}$ and $E'_{alk}=397$ mV for PGE and $K_H=2.21\times10^{-5}$ and $E'_{alk}=380$ mV for GCE. The K_H values translate into pK_a ($=-\log K_H$) values of 4.94 and 4.66, respectively. At the limiting alkaline potential, E'_{alk}, the difference in midpoint potential for the two electrodes, PGE and GCE, is 15 mV, that is, a significant difference between the redox potential for plastocyanin as measured by the two electrodes: PGE and GCE.

4.6. STM of poly-L-lysine on atomically flat gold

Imaging of the "edge-oriented" pyrolytic graphite electrode is difficult using scanning tunneling microscopy (STM) due to its uneven surface structure. Although numerous attempts were made to image poly-L-lysine on both edge-oriented and basal planar pyrolytic graphite, all were unsuccessful. However, good quality images were obtained

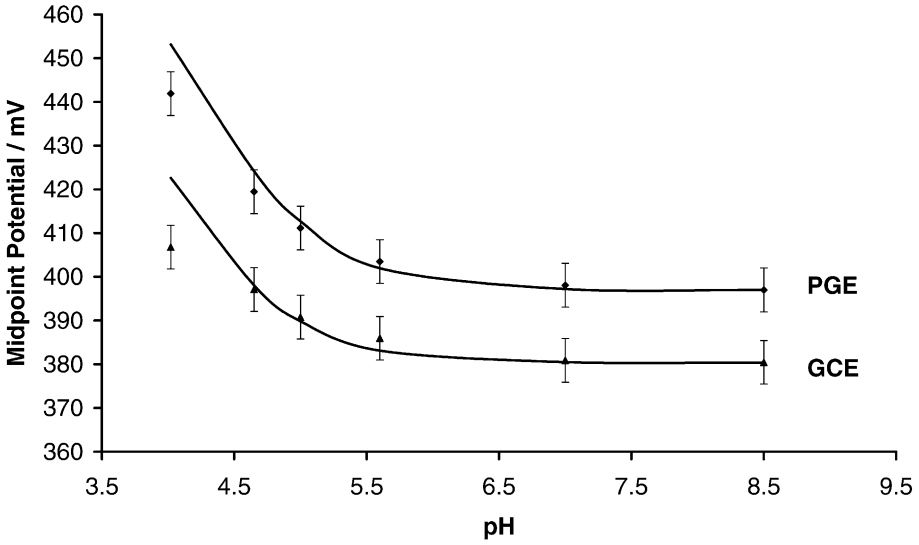

Fig. 5. Midpoint potentials, E_{mid}, plotted against pH for PGE and GC electrodes and poly-L-lysine promoter. Scan rate was 200 mV/s. The data points are experimental data and the solid line is a theoretical pH dependence curve-fit based on the Nernstian equation (see text).

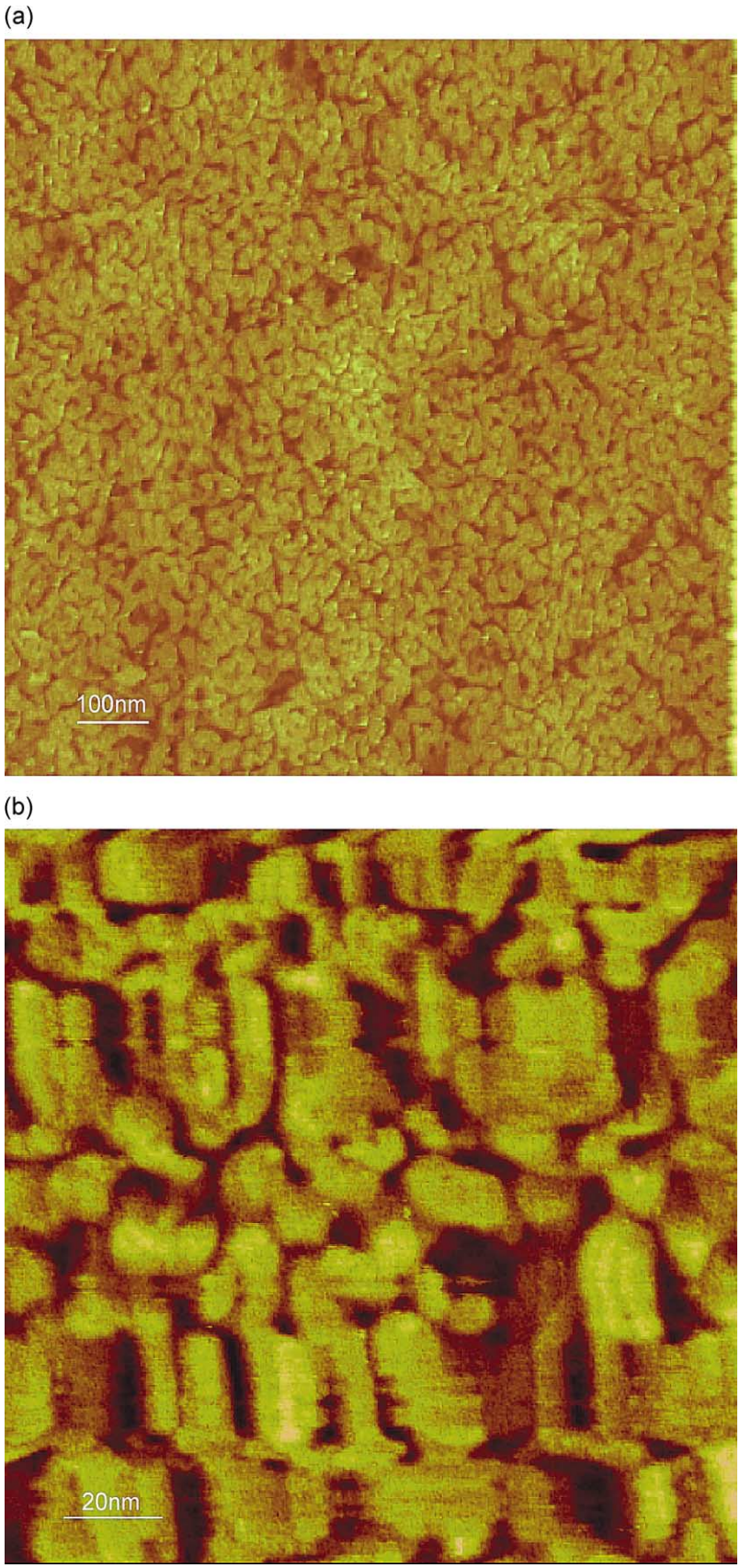

Fig. 6. STM images of poly-L-lysine on flat gold. (a) The larger image was recorded at 1.0×1.0 μm^2 while the same image has been magnified (b) to show a closer perspective (200×200 nm^2) of the poly-L-lysine.

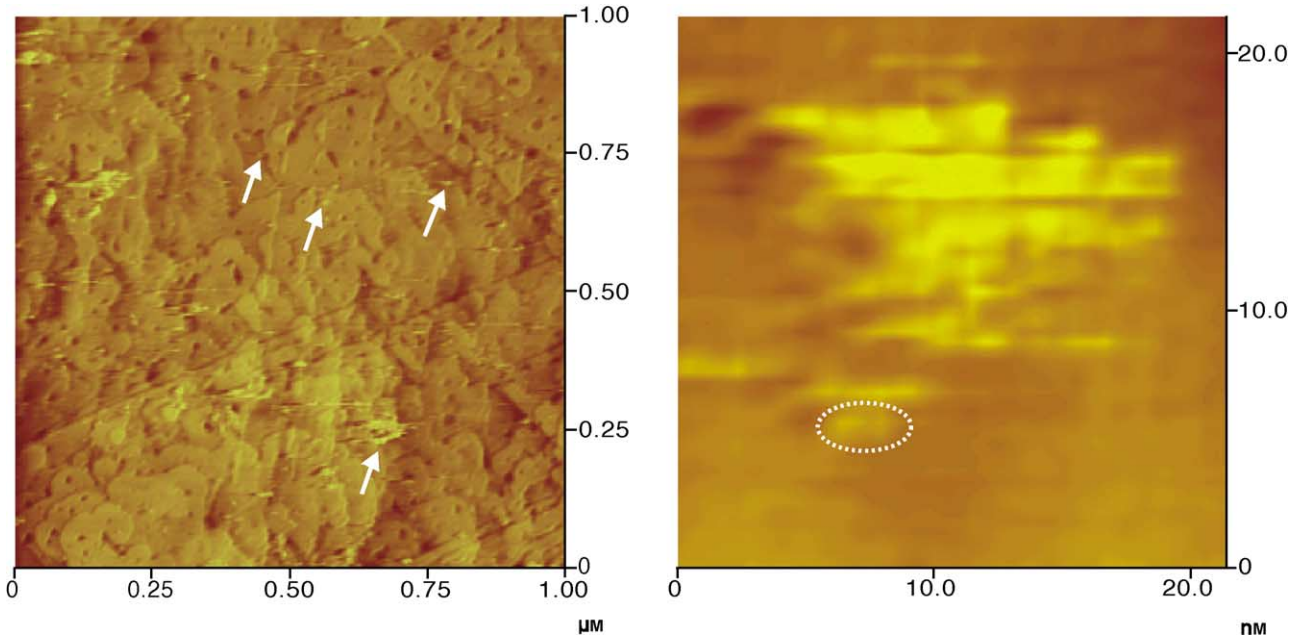

Fig. 7. STM images of plastocyanin on flat gold. The larger image (1.0×1.0 μm^2) shows isolated plastocyanin molecules as clusters of various sizes, as indicated by the arrows. The smaller scale image (20×20 nm^2) shows a single plastocyanin feature from a different sample. The ellipse highlights a small isolated plastocyanin cluster.

using atomically flat gold. The STM samples were prepared by the same procedure used to prepare the poly-L-lysine on gold surfaces for electrochemical measurements. The best images were obtained by washing the electrodes several times in water to obtain effectively a monolayer of promoter. Fig. 6 shows the STM images for atomically flat gold and those coated with poly-L-lysine. The highly ordered polymeric structure is readily observed revealing intra-peptide interactions that create ''secondary and tertiary'' structures within the promoter film.

4.7. STM of plastocyanin on atomically flat gold

One difficulty in imaging the plastocyanin/poly-L-lysine electrode combination was that the film thickness rapidly increases following the protein attachment so that no tunneling current can be detected. It was therefore not possible to obtain images of the protein orientation effects that we had anticipated. However, despite this limitation we obtained such good images of plastocyanin on a bare gold surface that we could identify single protein molecules of 1–2 nm in diameter. Fig. 7 shows a typical image of plastocyanin in which the protein solution was applied to the gold followed by several washes in water, air drying and imaging. These images were reproduced three times.

5. Discussion

Negatively charged metalloproteins, such as ferredoxins, cytochromes and plastocyanin, have been electrostatically immobilised to carbon electrodes and their electrochemistry investigated [1–4]. The nature of the promoter has been described as ''non-innocent'', resulting in shifts of 30 mV in some cases [7,8]. We included in this study seven different promoters, with a wide range of functional groups, size and overall charge. However, in this study (unlike others), we only used promoters that were large and polymeric. These promoters fall into two classes of biogenic amines: the antibiotic aminoglycosides (neomycin, tobramycin and geneticin) and the polyamines (poly-L-lysine, spermine, spermidine and polymyxin). The amine functional groups electrostatically bind the negatively charged oxides on the freshly polished PGE. The highest and lowest E_{mid} value for plastocyanin (Table 1) was found with the aminoglycosides, suggesting that the promoter was not the only contribution to the variation in E_{mid}.

Carbon electrodes are suitable electrodes for achieving a reversible response from plastocyanin in the presence of the promoter poly-L-lysine and we obtained reversible voltammetry at both the PGE and GCE. This is not unexpected, as carbon surfaces are well known to be suitable ''soft materials'' for proteins and enzymes. Other workers [7,8] have commented on the variation of E_{mid} using different promoters and with several metalloproteins; however, we believe that this study is the first time that an electrode dependence of midpoint potentials has been reported for plastocyanin.

The influence of promoter on the midpoint potential is shown in Fig. 2 for the PGE/promoter/plastocyanin combination. These data demonstrate that the selection of promoter can influence the midpoint potential by 10 mV and

that these data are reproducible within an error of 4 mV. It is interesting to note that poly-L-lysine provides a value midway within our range of promoters. Xiao et al. [8] have reported up to 20 mV difference between poly-L-lysine and hydrolysed chromium salts; however, this difference could well be due to the much smaller hydrolysed units (mono- and binuclear) formed by the chromium ions.

Of the two carbon electrodes used in this study, the edge-orientated pyrolytic graphite electrode provided the greater stability for poly-L-lysine/plastocyanin electrochemistry. Unlike the GCE, the PGE has exposed, oxidised phenyl groups that provide a good electrostatic attraction for the promoters, and it is envisaged that the promoter exists in the middle of an electrostatic "sandwich" comprising electrode and protein. The effect on the stability of the protein on the carbon electrodes is dramatic (see Fig. 4), with a sustained response on the PGE for an hour compared with minutes using the GCE. In contrast, the surface of the GCE differs in the graphitic microstructure compared to the PGE, and the density of carbon is much smaller [23].

The difference in midpoint potential for plastocyanin obtained using PGE versus GCE with poly-L-lysine is 15 mV. The magnitude of this effect remained unchanged over the pH range 4.0–8.5. The pH dependence of plastocyanin reduction potential is well known, and our dependence of E_{mid} with pH agrees with that obtained by others [11,15]. In addition, the values for K_H and E_{alk} agree well within an order of magnitude of values determined by others [17,24]. The influence of the electrode material on the pH dependence is unexpected because the midpoint potential at the GCE should present values more positive due to the smaller surface charge. However, the resulting pK_a values determined at each electrode are only affected to a small extent, although one half of a pH unit is not insignificant.

STM proved to be an invaluable tool for investigating the protein–electrode interface. We prepared atomically flat gold using vapour deposition as described elsewhere [25]. The flat gold surface contains a pattern due to the underlying structure of the mica-substrate onto which it prepared. The poly-L-lysine promoter covers the gold surface (Fig. 6) and the detailed structure can be imaged. The large scale image is 1000×1000 nm^2; the "brain-like" pattern is clearly apparent. The smaller image at 200×200 nm^2 reveals the intramolecular interactions within the poly-L-lysine polymer and the formation of some secondary and tertiary structure appears. Presumably, the intramolecular interactions result in the high density of charged amino moieties exposed at the surface resulting in this folding pattern and these units function as binding sites for the plastocyanin protein. Images of the plastocyanin directly on gold surfaces (Fig. 7) show the adsorbed plastocyanin molecules aggregate as various sized clusters ca. 14 nm (as indicated by the arrows). However, close examination of some of these smaller clusters (Fig. 7b) shows an isolated feature (circled) of the dimensions we would expect for a single or perhaps two plastocyanin molecules, that is, 2–4 nm in diameter. X-ray structure determinations of poplar plastocyanin [11] indicated that a single molecule has overall dimensions of $4.0\times3.2\times2.8$ nm^3. We are further investigating the promoter/protein interactions using atomic force microscopy (AFM) where the surface imaging does not rely on conduction of electrons (as for STM), and hence, imaging the thicker layers is possible.

In summary, the reversible electrochemistry of plastocyanin was achieved using both PGE and GCE in the presence of promoters. The nature of the promoter proved to be significant because the midpoint potential obtained varied depending on the promoter selected. The most stable response for plastocyanin was obtained using the combination of PGE/poly-L-lysine as the electrode and promoter. Using this combination, well-defined electrochemical data could be obtained for up to an hour. The type of electrode material used to measure the midpoint potentials could produce shifts in the potentials by up to 15 mV, but this was invariant over a range of pH. This electrode dependence of the redox process was also reflected in the derived pK_a values by almost one half of an order of magnitude. More work is clearly needed to explore these effects and influences on the electrode potentials determined for metalloproteins by direct electrochemistry; however, our results suggest caution should be applied in the interpretation of these data without detailed exploration of the electrochemical responses. The surface structure detailed by STM has provided insights into the promoter structure and further work will be valuable to understand electrochemical responses for proteins immobilised on these surfaces.

Acknowledgements

We thank Prof. Alex Hope for some of the plastocyanin, and Prof. Alan Bond for his comments and helpful discussions.

References

[1] A.M. Bond, Chemical and electrochemical approaches to the investigation of redox reactions of simple electron transfer metalloproteins, Inorg. Chim. Acta 226 (1994) 293–340.
[2] F.A. Armstrong, G.S. Wilson, Recent developments in faradic bioelectrochemistry, Electrochim. Acta 45 (2000) 2623–2645.
[3] F.A. Armstrong, H.A. Heering, J. Hirst, Reactions of complex metalloproteins studied by protein-film voltammetry, Chem. Soc. Rev. 26 (1997) 169–179.
[4] M. Fedurco, Redox reactions of heme-containing metalloproteins: dynamic effects of self-assembled monolayers on thermodynamics and kinetics of cyctochrome *c* electron-transfer reactions, Electrochim. Acta 209 (2000) 263–331.
[5] B. Shen, L.L. Martin, J.N. Butt, F.A. Armstrong, C.D. Stout, G.M. Jensen, P.J. Stephens, G.N. La Mar, C.M. Gorst, B.K. Burgess, *Azotobacter vinelandii* Ferredoxin I: aspartate 15 facilitates proton transfer to the reduced [3Fe4S] cluster, J. Biol. Chem. 268 (1993) 25928–25939.
[6] J.N. Butt, A. Sucheta, L.L. Martin, B. Shen, B.K. Burgess, F.A. Arm-

strong, Voltammetric study of proton-gated electron transfer in a Ferredoxin. Altering aspartate to asparagine blocks oxidation of the [3Fe4S] cluster of *Azotobacter vinelandii* Ferredoxin I, J. Am. Chem. Soc. 115 (1993) 12587–12588.

[7] D.D.N. McLeod, H.C. Freeman, I. Harvey, P.A. Lay, A.M. Bond, Voltammetry of plastocyanin at a graphite electrode: effects of structure, charge and electrolyte, Inorg. Chem. 35 (1996) 7156–7165.

[8] Z. Xiao, M.J. Lavery, A.M. Bond, A.G. Wedd, The dependence of reversible potentials on the form of modification of edge plane pyrolytic graphite electrodes in voltammetric studies on rubredoxin and ferredoxin form *Clostridium pasteurianum*, Electrochem. Commun. 1 (1999) 309–314.

[9] M. Rivera, M.A. Wells, F.A. Walker, Cation-promoted cyclic voltammetry of recombinant rat outer mitochondrial membrane cyctohrome b_5 at a gold electrode modified with β-mercaptopropionic acid, Biochemistry 33 (1994) 2161–2170.

[10] T. Sakurai, O. Ikeda, S. Suzuki, Direct electrochemistry of the blue copper proteins pseudoazurin, plantacyanin, and stellacyanin, Inorg. Chem. 29 (1990) 4715–4718.

[11] H.C. Freeman, M. Guss, Plastocyanin, in: A. Messerschmidt, et al. (Eds.), Handbook of Metalloproteins, vol. 2, Wiley, 2001, p. 1153.

[12] S.G. Taneva, U. Kaiser, A.A. Donchev, M.I. Dimitrov, W. Mantele, A. Muga, Redox-induced conformational changes in plastocyanin: an infrared study, Biochemistry 38 (1999) 9640–9647.

[13] G. Battistuzzi, M. Borsari, L. Loschi, M. Menziani, F. Righi, M. Sola, Redox thermodynamics of blue copper proteins, J. Am. Chem. Soc. 121 (1999) 501–506.

[14] G. Battistuzzi, M. Borsari, L. Loschi, M.C. Menziani, F. De Rienzo, M. Sola, Control of metalloprotein reduction potential: the role of electrostatic and solvation effects probed on plastocyanin mutants, Biochemistry 40 (2001) 6422–6430.

[15] D.G.A.H. de Silva, D. Beoku-Betts, P. Kyritsis, K. Govindaraju, R. Powls, N.P. Tomkinson, A.G. Sykes, Protein–protein cross-reactions involving plastocyanin, cyctochrome *f* and azurin: self-exchange rate constants and related studies with inorganic complexes, J. Chem. Soc. Dalton Trans., (1992) 2145–2151.

[16] T. Kohzuma, T. Inoue, F. Yoshizaki, Y. Sasakawa, K. Onodera, S. Nagatomo, T. Kitagawa, S. Uzawa, Y. Isobe, Y. Sugimura, M. Gotowda, Y. Kai, The structure and unusual pH dependence of plastocyanin from the fern *Dryopteris crassirhizoma*, J. Biol. Chem. 274 (1999) 11817–11823.

[17] F.A. Armstrong, H.A.O. Hill, B.N. Oliver, D. Whitford, Direct electrochemistry of the photosynthetic blue copper protein plastocyanin. Electrostatic promotion of rapid charge transfer at an edge-oriented pyrolytic graphite electrode, J. Am. Chem. Soc. 107 (1985) 1473–1476.

[18] B.A. Kuznetsov, N.A. Byzova, G.P. Shumakovich, L.E. Mazhorova, A.A. Mutuskin, Electrochemical investigation of binding sites of plantacyanin: blue, copper-containing protein of plants, Bioelectrochem. Bioenerg. 40 (1996) 249–255.

[19] T. Sakurai, F. Nose, T. Fujiki, S. Suzuki, Reduction and oxidation processes of blue copper proteins, azurin, pseudoazurin, umecyanin, stellacyanin, plantacyanin, and plastocyanin approached by cyclic and potential step voltammetries, Bull. Chem. Soc. Jpn. 69 (1996) 2855–2862.

[20] M. Wirtz, J. Klucik, M. Rivera, Ferredoxin-mediated electrocatylitic dehalogenation of haloalkanes by cytochrome $P450_{cam}$, J. Am. Chem. Soc. 122 (2000) 1047–1056.

[21] J. Haladjian, P. Bianco, L. Asso, F. Guerlesquin, M. Bruschi, Direct electrochemical reduction of spinach and *Desulfovibrio desulficams* Norway ferredoxins, Electrochim. Acta 32 (1986) 1513–1517.

[22] J.J. Davis, H.A.O. Hill, A.M. Bond, The application of electrochemical scanning probe microscopy to the interpretation of metalloprotein voltammetry, Coord. Chem. Rev. 200–202 (2000) 411–442.

[23] K. Shi, K. Shiu, Scanning tunneling microscopic and voltammetric studies of the surface structures of an electrochemically activated glassy carbon electrode, Anal. Chem. 74 (2002) 879–885.

[24] A.B. Hope, P. Valente, D.B. Matthews, Effects of pH on the kinetics of redox reactions in and around the cytochrome *bf* complex in an isolated system, Photosynth. Res. 40 (1994) 199–206.

[25] J. Mazurkiewicz, F. Mearns, D. Losic, C. Rogers, J.J. Gooding, J.G. Shapter, Cryogenic cleavage to yield ultraflat gold, Vac. Sci. Technol. A (2001), submitted for publication.